photonics

MDPI

Article

Resolving the Refractive Indices of Transparent and Translucent Liquids from the Spacings, Spatial Frequencies, and Directions of Interference Fringes

Qingli Jing *, Jiajian Wang, Jianglong Lei, Qi Wang, Jialing Chen, Jun Liu, Minglin Zhao, Jiantai Dou, Yuanxiang Wang and Youyou Hu

Department of Optoelectronic Information Science and Engineering, School of Science, Jiangsu University of Science and Technology, Zhenjiang 212100, China
* Correspondence: jingqingli@just.edu.cn

Abstract: In this work, we present a novel approach to resolve the refractive indices of transparent and translucent liquids from straight interference fringes. The optical path difference between the two arms of the Mach–Zehnder interferometer is first derived by assuming a reference plane wave interfering with a plane wave passing through a rectangular cuvette. The analytic expressions for the liquid refractive indices are then deduced, describing how the refractive index is related to the fringe spacings, spatial frequencies, and directions. The structure coefficients in the above formulas are determined from the fringe spacings and directions of the interference patterns of the empty cuvette and the cuvette filled with a liquid of a known refractive index. The NaCl solution and Coca Cola are adopted as the test examples to show experimentally the validity of the proposed method. There is good agreement between the refractive indices obtained from the fringe spacings and direction of a single interference pattern. The sensitivity and resolution of this method are dependent on the structure of the experimental systems and thus can be adjusted in a controlled manner. The proposed method is simple to implement and can be easily extended to other high precision optical interferometer systems.

Keywords: Mach–Zehnder interferometer; refractive index measurement; fringe spacing; fringe direction

Citation: Jing, Q.; Wang, J.; Lei, J.; Wang, Q.; Chen, J.; Liu, J.; Zhao, M.; Dou, J.; Wang, Y.; Hu, Y. Resolving the Refractive Indices of Transparent and Translucent Liquids from the Spacings, Spatial Frequencies, and Directions of Interference Fringes. *Photonics* **2024**, *11*, 782. https://doi.org/10.3390/photonics11090782

Received: 25 June 2024
Revised: 15 August 2024
Accepted: 20 August 2024
Published: 23 August 2024

1. Introduction

The refractive index is a key optical parameter for transparent and translucent materials. For liquids, it is closely related to parameters such as the wavelength of the light, the composition, the concentration, and the atmosphere temperature. The empirical expressions of the refractive index in terms of the concentration and temperature were derived for different liquids [1]. To measure the refractive indices of liquids, a variety of non-destructive, sensitive refractometers [2–4], reflectors [5,6], and other highly precise optical systems [7–9] have been proposed and designed.

There have been many reviews and research studies on utilizing optical interferometers to measure the indices of the refraction of liquids with high accuracy [10–14]. The Fabry–Perot interferometer is a good candidate due to its simplicity and versatility [15–17]. In addition, a single-element interferometer to measure the refractive index was designated by rotating a rectangular optical glass cell containing the sample liquid and air simultaneously and by calculating the interference fringe shift number from an interferogram. The measurement accuracy for the refractive index was up to 10^{-4} [14]. A dual scanning interferometric technique was applied to measure the temperature and concentration dependence of the refractive indices of liquids at concentrations smaller than 0.03% and at a high precision of the order of 1×10^{-7} for a 20 mm optical path [18]. High-precision refractive index

measurements of liquids were also carried out for wavelengths from 0.5 to 2 μm using Rayleigh interferometry [19].

Interferometers such as the Mach–Zehnder interferometer and the Michelson interferometer also play a prominent role in the field of precise measurement [20]. The fiber-based Mach–Zehnder interferometric sensors were applied to measure the refractive index and temperature of transparent liquids from the wavelength shift of the interference spectrum [21–24]. A very common strategy to obtain the refractive index of a sample is to apply fringe count techniques to measure the fringe shift due to the introduction of the sample in one arm of an interferometer. For example, a hybrid optical fiber interferometer, which consists of a Mach–Zehnder interferometer and a Michelson interferometer, was fabricated to achieve accurate measurement of the refractive indices of different liquids [25]. The standard deviation of the refractive index was about 10^{-5} RIU. The refractive index of water was 1.33157 at 25 °C when the wavelength was 632 nm, very close to 1.33158 in ref. [26]. The refractive index for NaCl solutions with concentrations smaller than 0.2% was measured. Using orbital angular momentum beams in a twisted Michelson interferometer opens the possibility for measurements of refractive index changes down to 10^{-6} RIU. The refractive index was measured from the rotation of interference patterns at very small concentrations [27]. The Michelson interferometer was applied to measure the refractive indices of liquids from measuring the fringe shifts, and the relationships among the solution concentration, temperature, and refractive index were established for different solutions [28]. In addition, high-resolution refractive index measurement was achieved by using differential interferometry, based on a white light Mach–Zehnder configuration [29] and by employing ultra-compact double-slot hybrid plasmonic waveguide as an active sensing arm in the interferometer [30].

A few inspired research works have reported interpreting the indices of the refraction of samples from the interference patterns of the free-space Mach–Zehnder interferometer. An early experiment was conducted to measure the local indices of the refraction of solutions from the relationship between the relative optical path length difference and the interference fringe bending [31]. The refractive index measurement error was about ±0.001 RIU. Recently, some researchers have reported employing a white light Mach–Zehnder interferometer to generate a series of interferograms to determine the refractive indices of materials [32]. A research work published in the same year has reported measuring the indices of the refraction of scintillation crystals from the width shift of interference patterns based on the Mach–Zehnder interferometer [33]. Their method is also suitable for measuring the indices of the refraction of liquids in a rectangular cuvette. A change in the direction of the interference stripes was witnessed in the interference patterns for different crystals. In this work, to understand the underlying physics in fringe spacing and direction changes, we propose a novel method to resolve the indices of the refraction of transparent and translucent liquids from the interference patterns of the Mach–Zehnder interferometer.

To verify the proposed method, the NaCl solution is adopted as one of the test examples to measure the refractive indices of NaCl solutions with various concentrations. For the NaCl solutions, large-scale experiments have been carried out to measure the refractive index at different wavelengths and temperatures. A brief review of the relevant works is given in the following sentences. The refractive indices of NaCl solutions was measured using the Abbe refractometer [34]. The fit curve for the refractive indices of NaCl solutions was $n = 0.0015c + 1.3327$ (R^2 = 0.9984) at 588 nm and at 28 ° C, with c representing the concentration of NaCl solutions. The Abbe refractometer was also used to measure the refractive indices of NaCl solutions of different concentrations and temperatures at the wavelength of 589.3 nm [1]. The empirical expression for the refractive index was $n = 1.3373 + 1.7682 \times 10^{-3}c - 5.8 \times 10^{-6}c^2 - 1.3531 \times 10^{-4}(T - 273.15) - 5.1 \times 10^{-8}(T - 273.15)^2$ with c representing the concentration and T representing the absolute temperature. Refs. [35,36] reported the refractive indices of NaCl solutions with concentrations ranging from 0 to 16.6667% in the spectral range of 0.3–1.0 μm at 20 °C and with concentrations from 0 to 4% at 22 °C and at the He-Ne laser wavelength, i.e., 632.8 nm, respectively. In ref. [28],

the relationships between the solution concentration, temperature, and refractive indices for NaCl solutions were established at 632.8 nm, with $n = 0.00012T + 0.00191c + 1.33095$, where T represents the temperature in Celsius. The refractive indices of NaCl solutions was measured for concentrations from 0 to 20% at 632.8 nm [37]. The fit curve for the refractive index was $n = 0.0018c + 1.3336$ (R^2 = 0.9993). The refractive indices of NaCl solutions was measured by using the image correlation coefficient under the He-Ne laser wavelength. The data obtained agreed well with that measured using the Abbe refractors [38]. In addition, the refractive indices of NaCl solutions was measured for concentrations from 0 to 1.8% at the wavelength of 850 nm [39], for concentrations from 5.5 to 33.2% at 543 nm and at 20 °C [40], for concentrations smaller than 0.03% [18], for concentrations up to 30% at 1550 nm [6], for concentrations from 0 to 25% at 1550 nm [41], for various concentrations at the wavelengths of 589 and 636.94 nm at 25 °C [14], and for very small concentrations at 532 nm [27].

This article is organized as follows. In Section 2, we illustrate in detail the derivation process of building up the analytic relations between the index of refraction and the fringe spacings, spatial frequencies, and directions of the interference patterns. In Section 3, the experimental results are presented and analyzed to verify the proposed method. Section 4 presents the conclusions of this study.

2. Theory and Methods

The schematic of the Mach–Zehnder interferometer measurement system is presented in Figure 1. A light beam from a He-Ne laser passing through a linear polarizer P is expanded and collimated using two lens L1 and L2. In this case, the light beam can be approximated by a monochromatic plane wave. Then, it is split into two paths by the beam splitter BS1. One light beam path first goes to mirror M2 and passes through the cuvette and then propagates to the beam splitter BS2. The other light beam path first goes to mirror M1 and is then reflected to the beam splitter BS2 to meet the first light beam. The photodetector CCD is placed after BS2 to capture the interference patterns generated due to the optical path difference between the two paths in the interferometer.

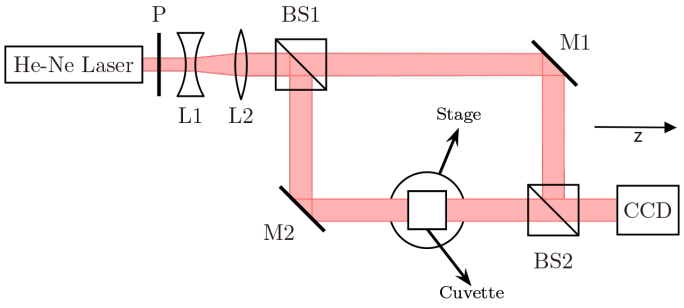

Figure 1. Schematic of the experimental system. P: linear polarizer; L1 and L2: two lens forming a beam expansion collimation system; BS1 and BS2: beam-splitting prisms; M1 and M2: reflective mirrors; cuvette placed on the stage: a setup to fill in liquids; CCD: the detector to record the interference patterns.

When the sensor surface of the CCD is placed perpendicular to the optical axis, i.e., the z axis in Figure 1, the optical path difference between the two paths is a linear function of position coordinates (x, y). When the cuvette is removed from the stage, the interference pattern on the CCD is simply from interference between two plane waves in the two paths. This optical path difference is

$$\Delta_1 = a_1 x + b_1 y + c_1. \quad (1)$$

This optical path difference also contains values from the beam splitters and the mirrors. Since they are highly uniform planar optical elements, the quadratic and higher-order polynomials in the optical path can be safely neglected. When the empty rectangular cuvette is placed on the stage, the interference pattern on the CCD will change due to an

additional optical path length introduced in this setup. Considering the good uniformity of the front and back quartz glass plates, the extra optical path difference induced by the empty cuvette is approximated by

$$\Delta_2 = a_2 x + b_2 y + c_2. \tag{2}$$

Thus, the total optical path length difference between the two paths in the Mach–Zehnder interferometer becomes

$$\Delta = \Delta_1 + \Delta_2 = (a_1 + a_2)x + (b_1 + b_2)y + (c_1 + c_2) = ax + by + c. \tag{3}$$

a and b are the structure coefficients that are responsible for the fringe spacings and directions of the interference pattern for the empty cuvette. When the cuvette is filled with liquids, as the front and back plates of the glass cuvette are not perfectly parallel to each other, there is always a very small angle between them due to machining errors, forming a liquid wedge. In fact, we take advantage of this property of the commercial rectangular quartz cuvette. The optical path difference from the liquid wedge is approximately by

$$\delta = c_a(n - n_a)x + c_b(n - n_a)y + c_l. \tag{4}$$

Here, c_a and c_b are independent of the liquids and are the structure coefficients for the liquid wedge in the cuvette. n is the index of refraction of the liquid to be measured, and $n_a = 1$ is the refractive index of air since the system is placed in free space. Therefore, when the cuvette contains liquids, the total optical path difference between the two paths is

$$\Pi = \Delta + \delta = (a + c_a(n - n_a))x + (b + c_b(n - n_a))y + (c + c_l). \tag{5}$$

By applying the constructive or destructive interference conditions ($\Pi = k\lambda$ or $\Pi = (k + 1/2)\lambda$ with k = 0, ±1, 0, ±2,... the number of wavelength between the two paths), we can obtain the fringe spacings between adjacent bright or dark fringes and the fringe directions of the interference pattern. For the empty cuvette, the fringe spacings in the x and y directions are

$$\begin{aligned} dx_0 &= \frac{\lambda}{|a|} = \frac{1}{f_{x0}}, \\ dy_0 &= \frac{\lambda}{|b|} = \frac{1}{f_{y0}}. \end{aligned} \tag{6}$$

in which f_{x0} and f_{y0} are the spatial frequencies of the interference fringes along the two directions. Thus, when the wavelength of the laser is known, after measuring the fringing spacings or spatial frequencies along the two perpendicular directions, the absolute value of structure coefficients a and b in Equation (3) for the optical path difference of the empty cuvette can be obtained. To determine the sign of these two coefficients, the direction of the interference fringes is required. If the angle of the fringes to the positive direction of the horizontal x axis is U_0, the fringe direction is described by the tangent of this angle

$$\tan(U_0) = -\frac{a}{b}. \tag{7}$$

Note that the sign of the tangent in Equation (7) indicates the direction of the interference fringes. When either a or b is initially set positive or negative, once the direction of the fringes is known, the sign of the other coefficient is definite. The fringe spacings dx and dy, the spatial frequencies f_x and f_y, and the tangent of the fringe direction $\tan(U)$ for the

interference fringes when the cuvette is filled with liquids can be similarly obtained from Equation (5), i.e.,

$$\begin{aligned} dx &= \frac{\lambda}{|a + c_a(n - n_a)|} = \frac{1}{f_x}, \\ dy &= \frac{\lambda}{|b + c_b(n - n_a)|} = \frac{1}{f_y}, \\ \tan(U) &= -\frac{a + c_a(n - n_a)}{b + c_b(n - n_a)}. \end{aligned} \tag{8}$$

To obtain the two unknown structure coefficients c_a and c_b, we can fill in the cuvette with a liquid of a known refractive index n_w. For example, the index of refraction of water is n_w = 1.3325 at the room temperature. After measuring the fringe spacings dx_1 and dy_1 (or the fringe spatial frequencies of f_{x1} and f_{y1}) of the interference fringes for the cuvette with water, c_a and c_b are obtained

$$\begin{aligned} c_a &= \frac{\pm\lambda/dx_1 - a}{n_w - n_a} = \frac{\pm\lambda f_{x1} - a}{n_w - n_a}, \\ c_b &= \frac{\pm\lambda/dy_1 - b}{n_w - n_b} = \frac{\pm\lambda f_{y1} - b}{n_w - n_b}. \end{aligned} \tag{9}$$

The fringe direction satisfies

$$\tan(U_1) = -\frac{a + c_a(n_w - n_a)}{b + c_b(n_w - n_a)}, \tag{10}$$

and is used to determine the sign in Equation (9). After determining all of the four structure coefficients a, b, c_a, and c_b, we can use this setup to measure the refractive index for a liquid from its fringe spacings dx_2 and dy_2 (or from fringe spatial frequencies f_{x2} and f_{y2}) and fringe direction $\tan(U_2)$. The analytic expressions for the liquid refractive indices are

$$\begin{aligned} n &= n_a + \frac{\pm\lambda/dx_2 - a}{c_a} = n_a + \frac{\pm\lambda f_{x2} - a}{c_a} \\ n &= n_a + \frac{\pm\lambda/dy_2 - b}{c_b} = n_a + \frac{\pm\lambda f_{y2} - b}{c_b} \\ n &= n_a - \frac{a + b\tan(U_2)}{c_a + c_b\tan(U_2)} \end{aligned} \tag{11}$$

with $\tan(U_2) = \pm dy_2/dx_2$. It is clear that the refractive index of a liquid is proportional to the spatial frequencies of the interference patterns. In principle, the above three equations will give us identical results for the index of refraction for a single liquid. However, due to the external noise, the simplification of the plane wave model and the limited resolution of the detectors, there is slight difference between these three values.

To show the influence of the liquid index of refraction on the fringe spacings (or spatial frequencies) and direction of the interference fringes, the simulation results for an illustrating example are presented in Figure 2 with a = 0.0002, b = −0.0002, c_a = 0.0005, c_b = 0.0005, n_a = 1, n_w = 1.3325, and n = 1.34, 1.36, and 1.38, respectively. The height and width of the each figure is 3600 × 3600 pixels. The pixel size is 2.4 × 2.4 μm.

In this example, the interference fringes of the empty cuvette in Figure 2a and the fringes of the water wedge in Figure 2b are perpendicular to each other. The combination of them for the cuvette filled with water and with the liquids of refractive indices of 1.34, 1.36, and 1.38 are shown in Figure 2c–f, respectively. The fringe spacings and the corresponding spatial frequencies in both the x and y directions and the fringe direction are changing when the cuvette is filled with liquids of different refractive indices. When the direction of the empty cuvette interference fringes are not parallel to that of the liquid wedge, both

the change in the fringe spacings and fringe direction can be observed when the index of refraction of the liquid varies. Sometimes, the naked eyes fail to detect this variation, but the highly precise photodetectors with a much larger resolving power can detect it.

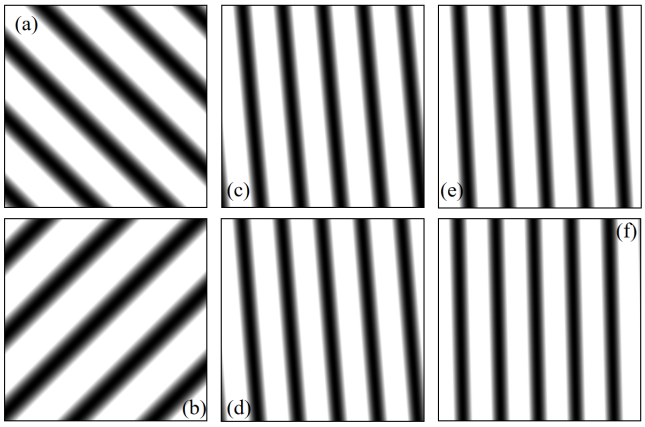

Figure 2. Simulated interference fringes for the empty cuvette (**a**) , the liquid wedge (**b**), the cuvette with water of refractive index of n_w = 1.3325 (**c**), and the cuvette with liquids of refractive indices of n = 1.34 (**d**), 1.36 (**e**), and 1.38 (**f**). The size of each figure is 3600 × 3600 pixels with a pixel size of 2.4 × 2.4 μm.

It is worth mentioning that the above derivation process is also valid for other interferometers. For example, when we consider the Michelson interferometer, the only difference is that the optical path difference between the two paths is twice of that for the Mach–Zehnder interferometer since the light beam passes through the cuvette twice in the sensing path. When the number of fringes of the empty cuvette and of the liquid wedge are comparable, the changes in the fringe direction are the most obvious. In the case of the two sets fringes for the empty cuvette and the liquid wedge are parallel, only the fringe spacings can be used to determine the indices of refraction for the liquids since the direction of the fringes are fixed. In the future, we will consider a more general case where the plane wave approximation of the optical path fails. In that case, we cannot expect very straight fringes with identical fringe widths and directions in the view field. By introducing a more complex optical path difference model, the possibility to simultaneously measure the local refractive indices of liquids is open.

3. Experimental Results and Discussion

To verify our proposed method of measuring the refractive indices of liquids, we conduct the relevant experiments to measure the indices of refraction of NaCl solutions by using the system in Figure 1. The atmosphere temperature is 23 ± 3 °C. The wavelength of the He-Ne laser is λ = 632.8 nm. The experimental system is shown in Figure 3. For the beam expansion and collimation system, the focal length of the concave lens is −9.8 mm and that of the convex lens is 100 mm. Thus, the magnification of this beam expander is about 100/9.8 ≈ 10 when the distance between the two lenses is around 99.2 mm. The dimension of the CCD is 5488 × 3672 pixels. Each pixel size is 2.4 × 2.4 μm. The quartz glass cuvette is rectangular in shape, and its optical path is around 10 mm. The distance between the front and back plates of the cuvette is also around 10 mm. To make the liquid in the cuvette stable in the small cuvette and to reduce the measurement error, the waiting time for each measurement after changing the liquid is at least 2 h.

To obtain the indices of refraction of the liquids from Equation (11), the four structure coefficients should be determined in advance. Among them, a and b are determined by the fringe spacings, spatial frequencies and direction of the interference pattern for the empty cuvette in Figure 4a from Equations (6) and (7). The interference pattern is closely related to the cuvette position on the stage and the two mirrors. To extract the fringe spacing from the

interference pattern, make sure a sufficient number of fringes appearing in the interference area. This is realized by adjusting the two mirrors. In addition, the number of the fringes should be controlled in a certain range; otherwise, the CCD cannot detect the variation in the fringe spacings from the interference patterns of liquids with very close concentrations. In this case, the sensitivity and accuracy of measuring the refractive index with this experimental system is very limited. The spatial frequencies of the interference fringes are obtained from the spectrum by taking the 2D Fourier transform of the corresponding interference patterns. Compared with the fast Fourier transform algorithm, the former Fourier transform method is applied to increase the precision of spatial frequency with the price of an increase in the computation time. After taking the reciprocal of the spatial frequencies, one can obtain the fringe spacings along the x and y directions. The advantage of this technique is noise insensitivity. In Figure 4a, the fringe spacings in x (horizontal) and y (vertical) direction are $dx_0 = 1.421$ mm and $dy_0 = 0.358$ mm, and the tangent of the fringe direction is $\tan(U_0) = 0.2517$. Substituting them into Equations (6) and (7), the structure coefficients for the empty cuvette are $a = 4.454 \times 10^{-4}$ and $b = -1.770 \times 10^{-3}$.

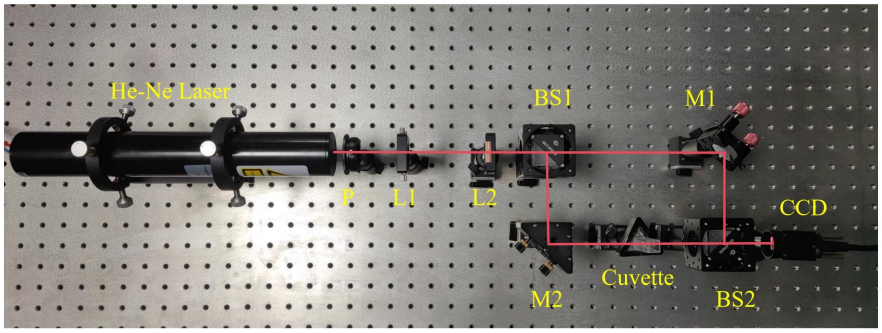

Figure 3. Experimental system constructed according to Figure 1. P: linear polarizer; L1 and L2: two lens forming a beam expansion collimation system; BS1 and BS2: beam-splitting prisms; M1 and M2: reflective mirrors; cuvette placed on the stage: a setup to fill in liquids; CCD: the detector to record the interference patterns.

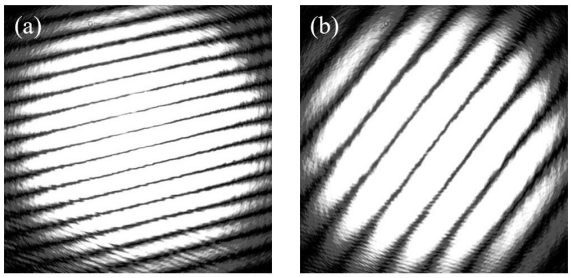

Figure 4. Experimental interference patterns for (**a**) the empty cuvette (**b**) and the cuvette with water n_w = 1.3315. The size of each figure is 2064 × 2060 pixels.

To obtain the structure coefficients of the liquid wedge, the interference pattern for the cuvette with a liquid of a known refractive index is required. In Figure 4b, the interference pattern for the cuvette filled with water is presented. The index of refraction of water was accurately measured at different wavelengths and temperatures [4,42,43]. We take n_w =1.3315 at the considered wavelength and at room temperature in this work. The fringe spacings are $dx_1 = 0.794$ mm and $dy_1 = 1.010$ mm, receptively. The tangent of the fringe direction is $\tan(U) = 1.2689$. Inputting them into Equation (8), we have the two structure coefficients for the liquid wedge $c_a = 1.061 \times 10^{-3}$ and $c_b = 3.441 \times 10^{-3}$. Since a and c_a are both positive, the fringe spacing in the x direction decreases as the index of refraction of the liquid increases. b and c_b have different signs, and the value of $b + c_b(n_w - n_a)$ becomes smaller than that of b. Thus, the fringe spacing in the y direction increases as the refractive index of the liquid increases. Meanwhile, the tangent of the fringe direction is increasing

with an increase in the refractive index, i.e., the fringes become more vertical for liquids with larger indices of refraction. Such trends are obvious in Figure 4.

After gathering all four structure coefficients and filling the cuvette with the liquids to be measured, the CCD was used to capture the corresponding interference patterns. The fringe spacings dx_2 and dy_2, spatial frequencies f_{x2} and f_{y2}, and direction $\tan(U_2)$ are first extracted from the interference patterns; then, Equation (11) was applied to obtain the indices of refraction of the liquids. The interference patterns for 5%, 10%, 15%, 20%, and 25% NaCl solutions are presented in Figure 5a–e. Here, the concentration refers to the weight fraction between NaCl and the NaCl solution. The refractive indices of these NaCl solutions together with the corresponding fringe spacings dx_2 and dy_2, spatial frequencies f_{x2} and f_{y2}, and direction $\tan(U_2)$ are presented in Table 1. $n(dx_2)$ and $n(dx_2)$ are the refractive indices obtained from the fringe spacings and spatial frequencies. $n(\tan(U_2)$ means the refractive index from the fringe direction. The second last row gives the average of the above three indices of refraction. In the last row, the data taken from ref. [38] are presented for comparison.

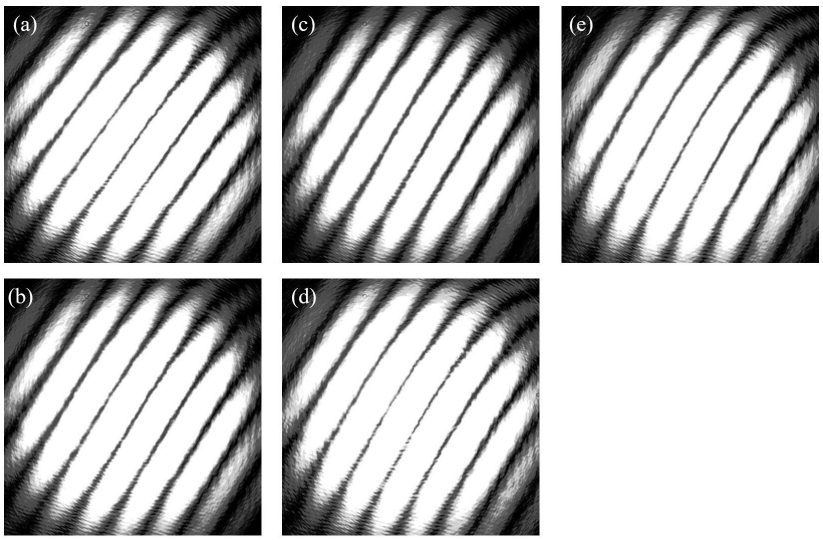

Figure 5. Experimental interference patterns for the cuvette filled with (**a**) 5%, (**b**) 10%, (**c**) 15%, (**d**) 20%, and (**e**) 25% NaCl solutions. The size of each figure is 2064 × 2060 pixels.

In Table 1, there is small variation between the three refractive indices for a NaCl solution. As we pointed out before, the error mainly comes from the external noise, the instability of the laser source, the plane wave approximation, the plane geometry assumption for the planar optical elements, and the limited resolving power of the CCD. Similar to ref. [33], the measurement accuracy of our method reaches around 10^{-3}.

To test the stability and repeatability of the measured refractive indices of NaCl solutions, we conduct a new experiment to measure the refractive indices of NaCl solutions by using the same cuvette. The atmosphere temperature is 27 ± 3 °C. The resultant interference patterns for the empty cuvette, cuvette filled with water, and cuvette filled with NaCl solutions with concentrations of 1, 5, 10, 15, 20, and 25% are shown in Figure 6. The interference pattern for the empty cuvette is very different from that in Figure 4, resulting in the interference patterns for water and NaCl solutions differing dramatically with those in Figure 5. From the fringe spacings or spatial frequencies of Figure 6a,b, the four structure coefficients can be obtained according to Equations (6)–(9). The fringe spacings and spatial frequencies of the interference pattern for the empty cuvette and water are shown in Table 2. They are used to calculate the structure coefficients for the empty cuvette and liquid wedge. The relevant data are also given in Table 2.

Table 1. Refractive indices and relevant data for NaCl solutions of different concentrations. dx_2 and dy_2 are the fringe spacings in the x and y directions. f_{x2} and f_{y2} are the corresponding fringe spatial frequencies. $\tan(U_2)$ is the tangent for the direction angle U_2 of interference fringes. $n(dx_2)$, $n(dy_2)$, and $n(\tan(U_2)$ are the refractive indices obtained from the fringe spacings and direction according to Equation (11). n is the average of the above three values. The values of n' are taken from ref. [38].

Concentration (%)	**5**	**10**	**15**	**20**	**25**
dx_2 (mm)	0.784	0.776	0.767	0.759	0.794
dy_2 (mm)	1.062	1.111	1.181	1.240	1.322
$\tan(U_2)$	1.354	1.431	1.539	1.633	1.760
f_{x2}	1275.3	1288.0	1303.2	1316.7	1331.4
f_{y2}	941.8	900.1	846.9	806.1	756.5
$n(dx_2)$	1.3409	1.3485	1.3575	1.3656	1.3743
$n(dy_2)$	1.3404	1.3481	1.3579	1.3654	1.3745
$n(\tan(U_2))$	1.3405	1.3481	1.3578	1.3654	1.3745
n	1.3406	1.3483	1.3577	1.3655	1.3744
n'	1.3415	1.3505	1.3595	1.3685	1.3767

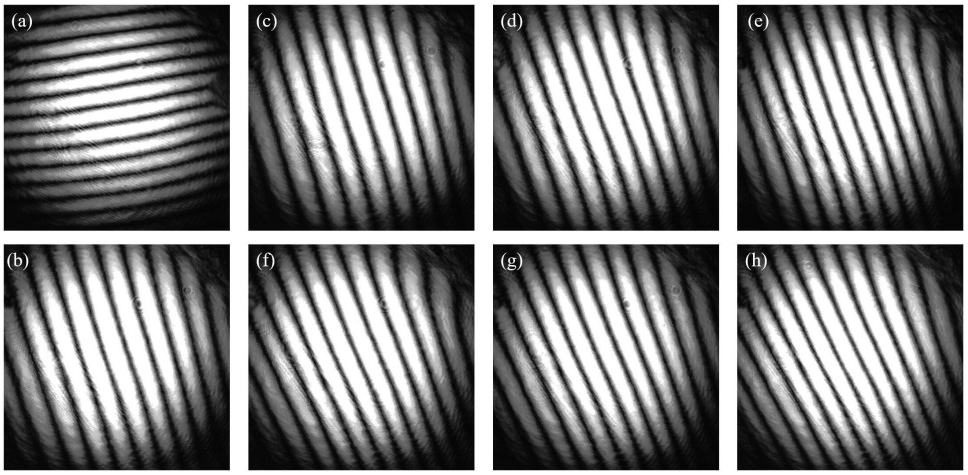

Figure 6. Interference patterns for empty cuvette (**a**), water (**b**), and NaCl solutions of concentrations 1% (**c**), 5% (**d**), 10% (**e**), 15% (**f**), 20% (**g**), and 25% (**h**). The size of each figure is 3500 × 3500 pixels.

Table 2. The four structure coefficients of the empty cuvette and liquid wedge. The fringe spacings and spatial frequencies for interference patterns of the empty cuvette and water are also given.

Fringe spacing (mm)	dx_0	dy_0	dx_1	dy_1
	4.164	0.673	0.878	2.744
Spatial frequencies	f_{x0}	f_{y0}	f_{x1}	f_{y1}
	240.1	1486.5	1139.1	364.4
Structure coefficients	a	b	c_a	c_b
	1.519×10^{-4}	-9.406×10^{-4}	1.716×10^{-3}	3.533×10^{-3}

In Table 2, it is clear that the four structure coefficients are different from that of the previous experiments. The slight difference between the structure coefficients of the liquid wedge indicates a slight change in the position of the cuvette for the new experiment. The fringe spacings, spatial frequencies, and directions of the interference patterns for NaCl solutions with different concentrations are given in Table 3. The refractive indices for these NaCl solutions are obtained by applying Equation (11). They are also listed in this table.

Table 3. Refractive indices and relevant data for NaCl solutions of different concentrations. dx_2 and dy_2 are the fringe spacings in the x and y directions. f_{x2} and f_{y2} are the corresponding fringe spatial frequencies. $\tan(U_2)$ is the tangent for the direction angle U_2 of interference fringes. $n(dx_2)$, $n(dy_2)$, and $n(\tan(U_2)$ are the refractive indices obtained from the fringe spacings and directions according to Equation (11). n is the average of the above three values. The values of n' are taken from ref. [38].

Concentration (%)	1	5	10	15	20	25
dx_2 (mm)	0.873	0.858	0.844	0.826	0.811	0.796
dy_2 (mm)	2.649	2.400	2.193	1.942	1.784	1.649
$\tan(U_2)$	−3.035	−2.796	−2.599	−2.352	−2.200	−2.073
f_{x2}	1145.6	1165.2	1185.1	1210.9	1233.5	1256.9
f_{y2}	377.5	416.7	456.0	514.8	560.6	606.4
$n(dx_2)$	1.3338	1.3411	1.3485	1.3580	1.3663	1.3748
$n(dy_2)$	1.3339	1.3409	1.3479	1.3584	1.3667	1.3750
$n(\tan(U_2))$	1.3338	1.3408	1.3478	1.3586	1.3667	1.3748
n	1.3338	1.3409	1.3481	1.3583	1.3666	1.3749
n'		1.3415	1.3505	1.3595	1.3685	1.3767

To make the relation between the refractive indices of NaCl solutions and the concentration more explicit and to better compare the data obtained by the two experiments, we draw the concentration and refractive index data points in Figure 7. Besides the linear fitting curves for the refractive index, the least squares method are plotted for the two experiments, and the function forms are $n = 1.3320 + 0.001706c$ and $n = 1.3320 + 0.001731c$ with c the concentration of the NaCl solution. The refractive indices of NaCl solutions obtained by the two individual experiments are very close to each other, confirming the stability and repeatability of the proposed method. To compare our results with that in ref. [38], the data taken from this reference are also plotted in Figure 7, with the fit curve for the refractive index reaching $n = 1.3330 + 0.001768c$. There is decent agreement between our experiments and the experiment in ref. [38]. The slight difference between the data of the experiments mainly comes from the difference in the atmosphere temperatures when the experiments were carried out. In principle, the refractive indices of both water and NaCl solutions at higher temperatures is smaller than the refractive indices at lower temperatures. Thus, it is apparent that the actuary of the proposed method is slightly influenced by the accuracy of the refractive index of water. The influence of the atmosphere temperature on the refractive indices of NaCl solutions is reflected in the deviation between the fitting curve and the measured data in Figure 7. When the concentration of the liquids is of concern, the relative trend of the refractive index matters, and the influence of the slight variation in the water index of refraction is reduced.

Here, we consider the sensitivity and resolution of our method. It is closely related to the structure of the experiment system, including the position of the cuvette and the positions of the two mirrors. The refractive indices of liquids are proportional to the spatial frequencies of the interference fringes according to Equation (11). This is confirmed in Figure 8, where the spatial frequencies in the x and y directions as a function of the refractive index (the data are taken from Tables 1 and 3) are plotted for the two experiments. The sensitivities are defined as the absolute values of the slopes of these curves. They are 1752/RIU in the x direction and 5454/RIU in the y direction for the first experiment, and 2694/RIU in the x direction and 5589/RIU in the y direction for the second experiment, respectively. Thus, the sensitivity of the latter experiment is improved. The resolution of the refractive index is defined as the ratio between the standard deviation of the spatial frequency and the sensitivity. After fitting the four curves in Figure 8, we have the root mean square error of 1.851 and 0.921 for f_{x2} and f_{y2} for the first experiment and 0.9408 and 0.6731 for f_{x2} and f_{y2} for the second experiment. Therefore, the resolutions for these four measurements are 0.0010, 0.00016, 0.00034, and 0.0012 RIU, respectively. The resolutions for these two experiments are not very high. The proposed method offers a new perspective to measure the refractive indices of liquids from the fringe spacings, spatial frequencies, and

directions of interference patterns. The advantage of this method is that the sensitivity and resolution can be adjusted and controlled. In addition, the degree of freedom on adjusting the two mirrors in the interferometer ensures a large measurement range of the refractive indices of liquids.

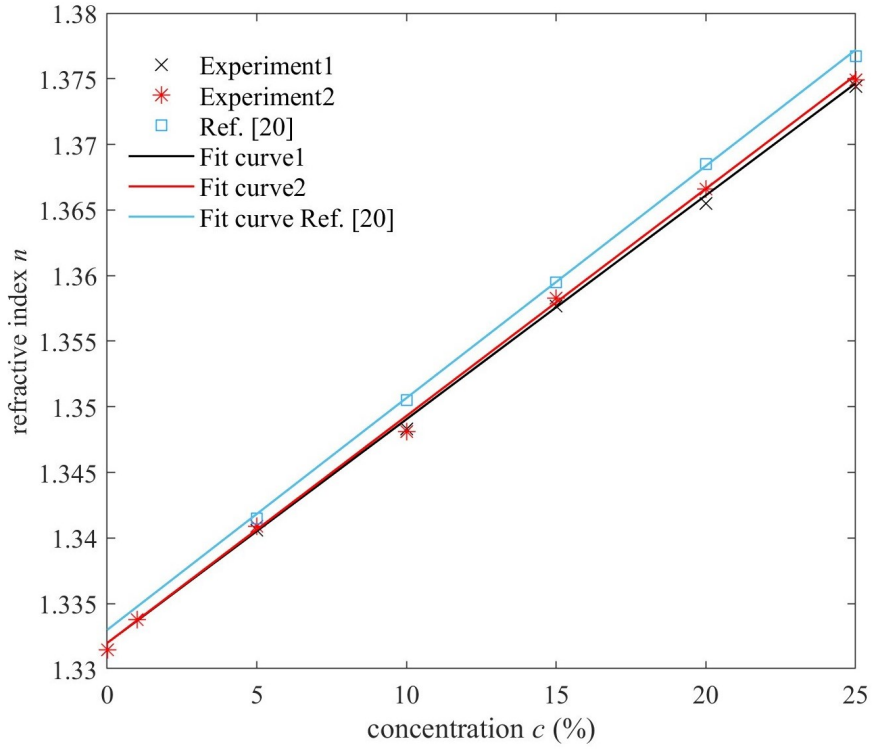

Figure 7. Measured refractive indices for NaCl solutions of different concentrations from the two experiments, marked by the asterisk and "x" symbols. The data marked by the square symbols are taken from ref. [20]. The sold lines are the linear fitting curves.

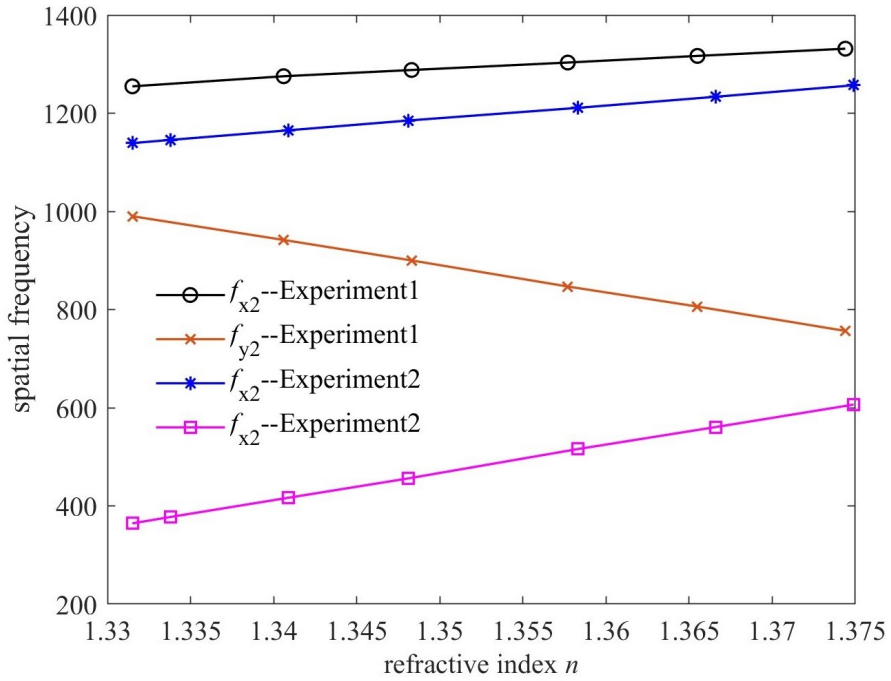

Figure 8. Spatial frequencies in the x and y directions as a function of the refractive indices for NaCl solutions for the two experiments.

Finally, to show the capacity of applying our method to measure the refractive indices of translucent liquids, we conducted an experiment on measuring the refractive index of Coca Cola by using the experimental system in Figure 3 at the atmosphere temperature of 28 ± 2 °C. The interference patterns for the empty cuvette, the cuvette filled with water, and the cuvette filled with Coca Cola are presented in Figure 9. To apply Equation (11) to obtain the refractive index of Coca Cola, we shall first calculate the structure coefficients of the empty cuvette and liquid wedge from the fringe spacings and spatial frequencies of Figure 9a,b. The corresponding results are given in Table 4. Since we adopted the same cuvette as the above two experiments, the structure coefficients for the liquid wedge in this experiment were very close to the results in Table 2. The slight difference between them comes from the slight difference in the positions of the cuvette between the two experiments. The fringe spacings, spatial frequencies, and directions of the interference pattern for Coca Cola in Figure 9c are $dx_2 = 0.742$ mm, $dy_2 = 3.882$ mm, f_{x2}=1348.4, $f_{y2} = 257.6$, and $\tan(U_2) = -5.234$, respectively. Thus, inputting the relevant data into Equation (11), we obtain the refractive indices of Coca Cola, i.e., $n(dx_2) = 1.3462$, $n(dy_2) = 1.3464$, and $n(\tan(U_2) = 1.3464$. The average of these three refractive indices is $n = 1.3463$, very close to 1.3472 in ref. [44], where the refractive index of Coca Cola was measured by the minimum deviation method at the wavelength of 650 nm and at room temperature, and close to 1.3487 and 1.3489 in ref. [45], where the refractive index of Coca Cola was measured using the Abbe refractometer and the designed apparatus at the wavelength of 532 nm and at the lab temperature of 20 ± 0.5 °C. It is the difference in the measurement wavelength and temperature that leads to the difference between our results and the results in the above-mentioned studies. Therefore, our method is applicable in measuring the real parts of the refractive indices of translucent liquids. It is beyond the capacity of our method to obtain the imaginary part of the refractive index of a translucent liquid to reflect the absorption of the liquid from the spacings, spatial frequencies, and directions of the interference fringes. In addition, for liquids with high turbidity, the applicability of our method is greatly reduced since no obvious interference fringes are generated due to the large scattering and absorption of light by the liquids.

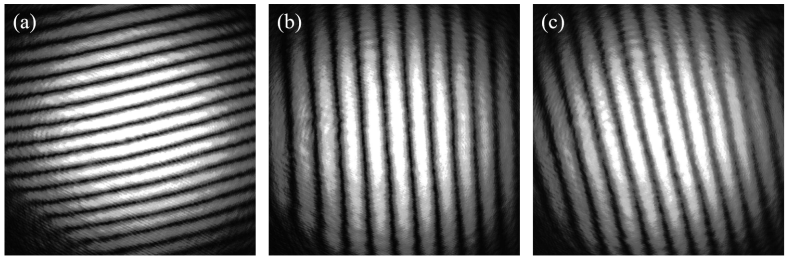

Figure 9. Interference patterns for empty cuvette (**a**), water (**b**), and Coca Cola (**c**). The size of each figure is 3500 × 3500 pixels.

Table 4. The four structure coefficients of the empty cuvette and liquid wedge. The fringe spacings and spatial frequencies for interference patterns of the empty cuvette and water are also given.

Fringe spacing (mm)	dx_0	dy_0	dx_1	dy_1
	2.362	0.536	0.764	6.017
Spatial frequencies	f_{x0}	f_{y0}	f_{x1}	f_{y1}
	423.3	1866.8	1309.0	166.2
Structure coefficients	a	b	c_a	c_b
	2.678×10^{-4}	-1.181×10^{-3}	1.691×10^{-3}	3.881×10^{-3}

4. Conclusions

In this work, we adopt a Mach–Zehnder interferometer to generate the interference patterns. A novel method is proposed to resolve the refractive indices of liquids from the fringe spacings, spatial frequencies, and directions of the interference patterns. For simplicity, the plane wave approximation is taken to assume a reference plane wave interfering with a plane wave passing through a rectangular cuvette. The optical path difference between the two arms of the interferometer comes from the optical path difference between two arms in free space, the optical path difference induced by the empty cuvette, and the liquid wedge in the cuvette. The analytic expressions between the refractive index and the spacings and between the refractive index and the fringe direction of the interference fringes are obtained. The structure coefficients in these expressions are determined from the interference patterns of the empty cuvette and the cuvette filled with a liquid of a known refractive index. Water is a good choice with a relatively stable index of refraction. To verify the proposed method, the NaCl solution is taken as the test example to show a measurement resolution of about 10^{-3}. Good agreement is achieved between the refractive index obtained from the fringe spacings and direction. We verified that the sensitivity and resolution of this method can be improved by adjusting the structure of the experimental system. In addition, the experiment on Coca Cola shows that this method can be also used to measure the refractive indices of translucent liquids. The proposed method is simple to implement and can be easily extended to other high-precision optical interferometer systems. Measurement precision will be further improved by taking a more complex model of the optical path difference, simultaneously measuring the local index of refraction for transparent and translucent materials possible.

Author Contributions: Conceptualization, Q.J. and J.W.; methodology, Q.J. and J.W.; validation, J.W., J.L. (Jianglong Lei), Q.W. and J.C. investigation, M.Z., J.D. and Y.H.; writing—original draft preparation, J.W. and Y.W.; writing—review and editing, Q.J. and J.L. (Jun Liu). All authors have read and agreed to the published version of the manuscript.

Funding: This work was funded by the National Natural Science Foundation of China under Grants No. 12104189, No. 12104190, and No. 11947110, and by Jiangsu Province Innovative and Entrepreneurial Doctoral Fund 2020 (Grant No. 1054902004).

Institutional Review Board Statement: Not applicable.

Informed Consent Statement: Not applicable.

Data Availability Statement: The data presented in this study are available from the corresponding author upon request.

Conflicts of Interest: The authors declare no conflicts of interest.

References

1. Tan, C.Y.; Huang, Y.X. Dependence of refractive index on concentration and temperature in electrolyte solution, polar solution, nonpolar solution, and protein solution. *J. Chem. Eng. Data* **2015**, *60*, 2827–2833. [CrossRef]
2. Cooper, P.R. Refractive-index measurements of liquids used in conjunction with optical fibers. *Appl. Opt.* **1983**, *22*, 3070–3072. [CrossRef]
3. Rheims, J.; Köser, J.; Wriedt, T. Refractive-index measurements in the near-IR using an Abbe refractometer. *Meas. Sci. Technol.* **1997**, *8*, 601. [CrossRef]
4. Pixton, B.M.; Greivenkamp, J.E. Automated measurement of the refractive index of fluids. *Appl. Opt.* **2008**, *47*, 1504–1509. [CrossRef]
5. Räty, J.; Keränen, E.; Peiponen, K.E. The complex refractive index measurement of liquids by a novel reflectometer apparatus for the UV-visible spectral range. *Meas. Sci. Technol.* **1998**, *9*, 95. [CrossRef]
6. Brientin, A.; Leduc, D.; Gaillard, V.; Girard, M.; Lupi, C. Numerical and experimental study of a multimode optical fiber sensor based on Fresnel reflection at the fiber tip for refractive index measurement. *Opt. Laser Technol.* **2021**, *143*, 107315. [CrossRef]
7. Longtin, J.P.; Fan, C.H. Precision laser-based concentration and refractive index measurement of liquids. *Microscale Thermophys. Eng.* **1998**, *2*, 261–272. [CrossRef]
8. Singh, S. Refractive index measurement and its applications. *Phys. Scr.* **2002**, *65*, 167. [CrossRef]

9. Vilitis, O.; Shipkovs, P.; Merkulov, D. Determining the refractive index of liquids using a cylindrical cuvette. *Meas. Sci. Technol.* **2009**, *20*, 117001. [CrossRef]
10. Yeh, Y.L. Real-time measurement of glucose concentration and average refractive index using a laser interferometer. *Opt. Lasers Eng.* **2008**, *46*, 666–670. [CrossRef]
11. Balling, P.; Mašika, P.; Křen, P.; Doležal, M. Length and refractive index measurement by Fourier transform interferometry and frequency comb spectroscopy. *Meas. Sci. Technol.* **2012**, *23*, 094001. [CrossRef]
12. Shakher, C.; Nirala, A.K. A review on refractive index and temperature profile measurements using laser-based interferometric techniques. *Opt. Lasers Eng.* **1999**, *31*, 455–491. [CrossRef]
13. Aydin, D.; Barnes, J.A.; Loock, H.P. In-fiber interferometry sensors for refractive index. *Appl. Phys. Rev.* **2023**, *10*, 011307. [CrossRef]
14. Zhang, T.; Feng, G.; Song, Z.; Zhou, S. A single-element interferometer for measuring refractive index of transparent liquids. *Opt. Commun.* **2014**, *332*, 14–17. [CrossRef]
15. Šantić, B.; Gracin, D.; Juraić, K. Measurement method for the refractive index of thick solid and liquid layers. *Appl. Opt.* **2009**, *48*, 4430–4436. [CrossRef]
16. Deng, M.; Tang, C.P.; Zhu, T.; Rao, Y.J.; Xu, L.C.; Han, M. Refractive index measurement using photonic crystal fiber-based Fabry-Perot interferometer. *Appl. Opt.* **2010**, *49*, 1593–1598. [CrossRef] [PubMed]
17. Liu, Y.-G.; Liu, X.; Zhang, T.; Zhang, W. Integrated FPI-FBG composite all-fiber sensor for simultaneous measurement of liquid refractive index and temperature. *Opt. Lasers Eng.* **2018**, *111*, 167–171. [CrossRef]
18. Postnikov, A. Dual scanning interferometric technique for measurements of the temperature and concentration dependence of the refractive index of liquids. *Meas. Sci. Technol.* **2020**, *32*, 015907. [CrossRef]
19. Chang, H.J.; Munera, N.; Lopez-Zelaya, C.; Banerjee, D.; Beadie, G.; Stryland, E.W.V.; Hagan, D.J. Refractive index measurements of liquids from 0.5 to 2 μm using Rayleigh interferometry. *Opt. Mater. Express* **2024**, *14*, 1253–1267. [CrossRef]
20. Bommareddi, R.R. Applications of optical interferometer techniques for precision measurements of changes in temperature, growth and refractive index of materials. *Technologies* **2014**, *2*, 54–75. [CrossRef]
21. Liu, W.; Wu, X.; Zhang, G.; Li, S.; Zuo, C.; Zhang, W.; Yu, B. Thin fiber-based Mach–Zehnder interferometric sensor for measurement ofliquid level, refractive index, temperature, and axial strain. *Appl. Opt.* **2020**, *59*, 1786–1792. [CrossRef]
22. Wo, J.; Wang, G.; Cui, Y.; Sun, Q.; Liang, R.; Shum, P.P.; Liu, D. Refractive index sensor using microfiber-based Mach–Zehnder interferometer. *Opt. Lett.* **2012**, *37*, 67–69. [CrossRef]
23. Wang, Y.; Yang, M.; Wang, D.N.; Liu, S.; Lu, P. Fiber in-line Mach-Zehnder interferometer fabricated by femtosecond laser micromachining for refractive index measurement with high sensitivity. *J. Opt. Soc. Am. B* **2010**, *27*, 370–374. [CrossRef]
24. Lu, P.; Men, L.; Sooley, K.; Chen, Q. Tapered fiber Mach–Zehnder interferometer for simultaneous measurement of refractive index and temperature. *Appl. Phys. Lett.* **2009**, *94*, 131110. [CrossRef]
25. Suhadolnik, A. An optical fibre interferometric refractometer. *Meas. Sci. Technol.* **2007**, *18*, 1205. [CrossRef]
26. Schiebener, P.; Straub, J.; Levelt Sengers, J.M.H.; Gallagher, J.S. Refractive index of water and steam as function of wavelength, temperature and density. *J. Phys. Org. Chem.* **1990**, *19*, 677–717. [CrossRef]
27. Kerschbaumer, N.M.; Fochler, L.I.; Reichenspurner, M.; Rieger, S.; Fedoruk, M.; Feldmann, J.; Lohmüller, T. Twisted light Michelson interferometer for high precision refractive index measurements. *Opt. Express* **2022**, *30*, 29722–29734. [CrossRef] [PubMed]
28. Shang, J.; Ping, L.; Ling, Y.; Chen, M.; Wang, Z.; Liu, M. A instrument for measuring solution concentration. *Opt. Rev.* **2023**, *30*, 310–321. [CrossRef]
29. Gouveia, C.; Zibaii, M.; Latifi, H.; Marques, M.J.; Baptista, J.; Jorge, P.A. High resolution temperature independent refractive index measurement using differential white light interferometry. *Sens. Actuators B Chem.* **2013**, *188*, 1212–1217. [CrossRef]
30. Sun, X.; Dai, D.; Thylén, L.; Wosinski, L. High-sensitivity liquid refractive-index sensor based on a Mach-Zehnder interferometer with a double-slot hybrid plasmonic waveguide. *Opt. Express* **2015**, *23*, 25688–25699. [CrossRef]
31. Cole, T.; Kathman, A.; Koszelak, S.; Mcpherson, A. Determination of local refractive index for potein and virus crystals in solution by Mach-Zehnder interferometry. *Anal. Biochem.* **1995**, *231*, 92–98. [CrossRef] [PubMed]
32. Drouillard, N.G.; Hammond, T.J. Measurement of dispersion and index of refraction of 1-decanol with spectrally resolved white light interferometry. *Opt. Express* **2022**, *30*, 39407–39416. [CrossRef] [PubMed]
33. Liu, X.; Long, J.; Ding, Y.; Hu, Y.; Du, Z.; Xu, B.; Deng, D. Measuring the refractive index of scintillation crystal with a Mach-Zehnder interferometer. *Opt. Contin.* **2022**, *1*, 909–918. [CrossRef]
34. Sudarsono, S.; Yudoyono, G.; Prajitno, G.; Sunarno, H.; Rohedi, A.Y.; Indarto, B.; Pramono, Y.H. Detection of salinity in the process of heating seawater by using a directional coupler of the multimode plastic optical fiber with a plane mirror as a reflector. *J. Opt.* **2020**, *49*, 48–52. [CrossRef]
35. Wang, C.C.; Tan, J.Y.; Liu, L.H. Wavelength and concentration-dependent optical constants of NaCl, KCl, $MgCl_2$, $CaCl_2$, and Na_2SO_4 multi-component mixed-salt solutions. *Appl. Opt.* **2017**, *56*, 7662–7671. [CrossRef]
36. Tengesdal, Ø.A. Measurement of Seawater Refractive Index and Salinity by Means of Optical Refraction. Master's Thesis, University of Bergen, Bergen, Norway, 2012.
37. Singh, V.; Jaswal, B.B.; Kumar, V.; Prakash, R.; Rai, P. Application of He-Ne Laser to Study of the Variation of Refractive Index of Liquid Solutions with the Concentration. *J. Integr. Sci. Technol.* **2013**, *1*, 13–18.

38. Xie, X.; Chen, J.; Zhou, M.; Xu, J.; Zheng, Z.; Yang, J.; Luo, J.; Zhong, Y. A method of liquid refractive index measurement based on image correlation coefficient. *J. Phys. Conf. Ser.* **2024**, *2724*, 012030. [CrossRef]
39. Khozeymeh, F.; Razaghi, M. Sensitivity and intrinsic limit of detection improvement in a photonic refractive-index sensor. *Optik* **2021**, *247*, 167844. [CrossRef]
40. Hsu, C.C.; Liu, T.S. Refractive index measurement using laser diffractometer. In Proceedings of the 2011 Fifth International Conference on Sensing Technology, Palmerston North, New Zealand, 28 November–1 December 2011; pp. 370–375. [CrossRef]
41. Moeinimaleki, K.; Habibzadeh-Sharif, A.; Ahmadpour, A.; Bahrami-Chenaghlou, F. Design and analysis of Si photonic NaCl sensors based on suspended microdisk resonators. *Phys. Scr.* **2024**, *99*, 055507. [CrossRef]
42. Harvey, A.H.; Gallagher, J.S.; Sengers, J.M.H.L. Revised formulation for the refractive index of water and steam as a function of wavelength, temperature and density. *J. Phys. Chem. Ref. Data* **1998**, *27*, 761–774. [CrossRef]
43. Daimon, M.; Masumura, A. Measurement of the refractive index of distilled water from the near-infrared region to the ultraviolet region. *Appl. Opt.* **2007**, *46*, 3811–3820. [CrossRef] [PubMed]
44. Belay, A.; Assefa, G. Concentration, wavelength and temperature dependent refractive index of sugar solutions and methods of determination contents of sugar in soft drink beverages using laser lights. *J. Lasers Opt. Photonics* **2018**, *5*, 1000187.
45. Xu, M.; Ren, J.; Miao, R.; Zhang, Z. Nonintrusive measurement of the liquid refractive index by using properties of the cuvette wall. *Appl. Opt.* **2016**, *55*, 8101–8106. [CrossRef] [PubMed]